Am J Physiol Heart Circ Physiol 291: H274–H282, 2006.
First published February 10, 2006; doi:10.1152/ajpheart.01064.2005.

Production of NAADP and its role in Ca^{2+} mobilization associated with lysosomes in coronary arterial myocytes

Fan Zhang,[1] Guo Zhang,[1] Andrew Y. Zhang,[1] Matthew J. Koeberl,[2] Eryn Wallander,[2] and Pin-Lan Li[1]

[1]*Department of Pharmacology and Toxicology, Medical College of Virginia, Virginia Commonwealth University, Richmond, Virginia; and* [2]*Department of Pharmacology and Toxicology, Medical College of Wisconsin, Milwaukee, Wisconsin*

Submitted 7 October 2005; accepted in final form 27 January 2006

Zhang, Fan, Guo Zhang, Andrew Y. Zhang, Matthew J. Koeberl, Eryn Wallander, and Pin-Lan Li. Production of NAADP and its role in Ca^{2+} mobilization associated with lysosomes in coronary arterial myocytes. *Am J Physiol Heart Circ Physiol* 291: H274–H282, 2006. First published February 10, 2006; doi:10.1152/ajpheart.01064.2005.—The present study was designed to determine the production of nicotinic acid adenine dinucleotide phosphate (NAADP) and its role associated with lysosomes in mediating endothelin-1 (ET-1)-induced vasoconstriction in coronary arteries. HPLC assay showed that NAADP was produced in coronary arterial smooth muscle cells (CASMCs) via endogenous ADP-ribosyl cyclase. Fluorescence microscopic analysis of intracellular Ca^{2+} concentration ($[Ca^{2+}]_i$) in CASMCs revealed that exogenous 100 nM NAADP increased $[Ca^{2+}]_i$ by 711 ± 47 nM. Lipid bilayer experiments, however, demonstrated that NAADP did not directly activate ryanodine (Rya) receptor Ca^{2+} release channels on the sarcoplasmic reticulum. In CASMCs pretreated with 100 nM bafilomycin A1 (Baf), an inhibitor of lysosomal Ca^{2+} release and vacuolar proton pump function, NAADP-induced $[Ca^{2+}]_i$ increase was significantly abolished. Moreover, ET-1 significantly increased NAADP formation in CASMCs and resulted in the rise of $[Ca^{2+}]_i$ in these cells with a large increase in global Ca^{2+} level of 1,815 ± 84 nM. Interestingly, before this large Ca^{2+} increase, a small Ca^{2+} spike with an increase in $[Ca^{2+}]_i$ of 529 ± 32 nM was observed. In the presence of Baf (100 nM), this ET-1-induced two-phase $[Ca^{2+}]_i$ response was completely abolished, whereas Rya (50 μM) only markedly blocked the ET-1-induced large global Ca^{2+} increase. Functional studies showed that 100 nM Baf significantly attenuated ET-1-induced maximal constriction from 82.26 ± 4.42% to 51.80 ± 4.36%. Our results suggest that a lysosome-mediated Ca^{2+} regulatory mechanism via NAADP contributes to ET-1-induced Ca^{2+} mobilization in CASMCs and consequent vasoconstriction of coronary arteries.

β-nicotinamide adenine dinucleotide phosphate; adenosine 5′-diphosphate-ribosyl cyclase; coronary artery; vascular smooth muscle

NICOTINIC ACID (NA) adenine dinucleotide phosphate (NAADP) is produced from $NADP^+$ by a replacement of its nicotinamide (Nicot) group with NA via ADP-ribosyl cyclase or its mammalian homologue CD38 (1). NAADP was first identified to mobilize Ca^{2+} in sea urchin eggs (40), and recently this signaling nucleotide has been shown to act as an endogenous regulator of intracellular Ca^{2+} in a wide variety of cell types from plants to animals, thereby participating in the regulation of cell functions, such as fertilization, cell proliferation and differentiation, insulin secretion, and nitric oxide signaling, as well as muscle constriction (33, 37, 42, 50). In contrast to the well-characterized D-*myo*-inositol 1,4,5-trisphosphate [$Ins(1,4,5)P_3$] and cyclic ADP ribose (cADPR)/Ca^{2+} signaling pathways (38, 52), the mechanisms mediating NAADP/Ca^{2+} signaling still remain enigmatic. Recent studies (3, 7) from different tissues or cells have suggested that NAADP is a novel secondary messenger to mobilize intracellular Ca^{2+} via a mechanism completely different from $Ins(1,4,5)P_3$ and cADPR. In sea urchin egg homogenates, for example, NAADP-induced Ca^{2+} mobilization undergoes homologous desensitization but does not affect subsequent Ca^{2+} release by $Ins(1,4,5)P_3$ or cADPR, the inhibitors of $Ins(1,4,5)P_3$ or cADPR, and the Ca^{2+} pump blocker of the $Ins(1,4,5)P_3$/cADPR stores have no effects on the NAADP-induced Ca^{2+} release (15).

Although this NAADP-mediated Ca^{2+} signaling pathway has distinctive characteristics from that of other intracellular Ca^{2+} messengers by targeting different Ca^{2+} storing organelles, there is accumulating evidence that the coordination of action of NAADP with other Ca^{2+} mobilizing messengers in the Ca^{2+} cascade events is importantly involved in the regulation of intracellular Ca^{2+} levels (7, 9). For example, in pancreatic acinar cells, NAADP evoked a local Ca^{2+} release in the apical granular pole, and this local Ca^{2+} spike could be propagated to a global Ca^{2+} wave under the concerted action of cADPR and $Ins(1,4,5)P_3$ (9). In other studies (15, 34, 57) using pulmonary arterial smooth muscle cells, it has been revealed that local Ca^{2+} could be sequestered to produce a global Ca^{2+} wave by Ca^{2+} release from the sarcoplasmic reticulum (SR) via Ca^{2+}-induced Ca^{2+} release (CICR) mechanism, which is related to the activation of $Ins(1,4,5)P_3$ receptors (IP_3Rs) and ryanodine (Rya) receptors on the SR. It seems that NAADP serves as a trigger of global Ca^{2+} response to different agonists, which was named in some reports as a two-pool mechanism for the regulation of intracellular Ca^{2+} levels (5, 13). With a consideration of a wide variety of cellular processes are regulated by changes of intracellular Ca^{2+} concentrations, from fertilization to cell death, it is possible that this spatiotemporal Ca^{2+} pattern related to NAADP may importantly contribute to the regulation of different cell functions, either through its action as second messenger or via its activity to synchronize the actions of other second messengers.

Previous studies from our laboratory and by others have demonstrated that cADPR is an important Ca^{2+}-signaling second messenger, which importantly contributes to the regulation of coronary vascular tone and vasomotor response. It has been reported that an ADP-ribosyl cyclase-mediated enzymatic pathway is present in coronary arterial smooth muscle, which

Address for reprint requests and other correspondence: P.-L. Li, Dept. of Pharmacology and Toxicology, Medical College of Virginia, Virginia Commonwealth Univ., 410 N. 12th St., PO Box 980613, Richmond, VA 23298 (e-mail: pli@mail1.vcu.edu).

The costs of publication of this article were defrayed in part by the payment of page charges. The article must therefore be hereby marked "*advertisement*" in accordance with 18 U.S.C. Section 1734 solely to indicate this fact.

is responsible for the production of cADPR under resting conditions or in response to different stimuli (22, 43, 59). Given that ADP-ribosyl cyclase is also responsible for the conversion of $NADP^+$ into NAADP, we wondered whether NAADP may also be produced in coronary arterial smooth muscle and involved in the regulation of coronary arterial tone or vasomotor response and how this new signaling nucleotide participates in the regulation of intracellular Ca^{2+} concentration ($[Ca^{2+}]_i$) in coronary arterial smooth muscle cells (CASMCs). In addition, it is also imperative to know whether NAADP can interact with other intracellular second messengers to regulate cellular Ca^{2+} responses. To answer these questions, the present study first characterized the production of NAADP in coronary arterial smooth muscle preparation. Using HPLC analysis, we determined the conversion of $NADP^+$ into NAADP by coronary homogenates, microsomes, and cytosols. We then addressed whether NAADP can induce Ca^{2+} release response in coronary arterial muscle cells using fluorescence imaging techniques and ultrasound microbubble intracellular delivery method. In reconstituted lipid bilayer with purified SR proteins, we examined whether NAADP changed Rya receptor (RyR) activity. To determine the role of endogenously produced NAADP in mediating the response to agonists, we tested the effects of endothelin-1 (ET-1) on the production of NAADP and analyzed the Ca^{2+} release and vasomotor responses to ET-1 before and after inhibition of lysosomal function, which has been reported to serve as a target for the signaling action of NAADP.

MATERIALS AND METHODS

Culture of CASMCs. The bovine CASMCs were cultured as described previously (44, 46). Briefly, the vessels were first rinsed with 5% FBS in medium 199 containing 25 mM HEPES with 1% penicillin, 0.3% gentamycin, and 0.3% nystatin and then cut into segments, and the lumen was filled with 0.4% collagenase in medium 199. After 30 min of incubation at 37°C, the vessels were flushed with medium 199. The strips of denuded arteries were placed into gelatin-coated flasks with medium 199 containing 10% FBS with 1% L-glutamine, 0.1% tylosin, and 1% penicillin-streptomycin. CASMCs migrated to the flasks within 3–5 days. Once growth was established, the vessels were removed and cells were grown in medium 199 containing 20% FBS. The identification of CASMCs was based on positive staining by an anti-α-actin antibody.

HPLC analysis of NAADP production in coronary arterial muscle. Bovine coronary arterial homogenates were prepared as we described previously (44). Briefly, bovine hearts were obtained from a local slaughterhouse. The left anterior descending artery was dissected and homogenized in ice-cold HEPES buffer (pH 7.4), which contained (in mM) 20 HEPES, 1 EDTA, 255 sucrose, 1 PMSF, 1 Na_3VO_4, and 1 mg/ml leupeptin, and to 40 ml of HEPES buffer were added 1 tablet of complete proteinase inhibitor cocktail (Roche Diagnostics). After centrifugation of the homogenate at 6,000 *g* for 5 min at 4°C, the supernatant containing the membrane protein and cytosolic components was aliquoted and frozen in liquid N_2 and termed the homogenate. Microsomes and cytosols were prepared by a differential centrifugation of the homogenate at 10,000 *g* for 20 min and at 100,000 *g* for 90 min, respectively. The pellet was named the microsomal fraction, whereas the supernatant was named the cytosolic fraction. To determine the production of NAADP, different amounts of homogenates (10, 50, 100, and 200 μg) were incubated for 30 min with 1 mM $NADP^+$ and 30 mM NA at 37°C in HEPES buffer containing (in mM) 20 HEPES, 1 EDTA, and 255 sucrose (pH = 4.5), with a total reaction volume of 0.1 ml. Before HPLC analysis, the reaction mixtures were centrifuged at 4°C with the use of an Amicon microultrafilter at 13,000 rpm for 15 min to remove the proteins. The reaction products in the ultrafiltrate were analyzed on a Supelcosil LC-18 (3 μm, 4.6 × 150 mm) with a Supelcosil LC-18 guard column (5 μm, 4.6 × 20 mm; Supelco, Bellefonte, PA) by the use of a Hewlett-Packard 1090L solvent delivery system and a 1040A photodiode array detector (Hewlett-Packard, Avondale, PA). Data were collected and analyzed with a Hewlett-Packard Chemstation. Mobile phase consisted of 5 mM potassium dihydrogen phosphate (pH 5.5) containing 5 mM tetrabutylammonium dihydrogen sulfate (*solvent A*) and acetonitrile (*solvent B*). The nucleotides were separated in *solvent A* with a gradient of 0–25% *solvent B* over 12 min and then to 100% *solvent B* over the next 4 min. *Solvent B* was held constant for 4 min and then returned to 100% *solvent A* for the last 10 min. The flow rate was 0.8 ml/min. The column eluate was monitored at 254 nm. Peak identities were confirmed by comigration and absorbance spectra compared with the known standards. Quantitative measurements were performed by comparison of known concentration of standards.

To determine which part of the CASMCs had higher enzymatic activity regarding NAADP synthesis, the microsome and cytosol of coronary arterial preparations were made for the NAADP conversion experiments by HPLC analysis.

Fluorescence measurement of $[Ca^{2+}]_i$ in CASMCs. A fluorescence image analysis system was used to determine $[Ca^{2+}]_i$ in the primary cultures of CASMCs with fura-2 acetoxymethyl ester (fura-2) as an indicator (60). Having been loaded with 10 μM fura-2 at room temperature for 30 min, the cells were washed three times with Ca^{2+}-free Hanks' buffer. A fluorescence ratio of excitation at 340 nm to that at 380 nm (F340/F380) was determined after background subtraction, and $[Ca^{2+}]_i$ was calculated by using the following equation: $[Ca^{2+}]_i = K_d\beta[(R - R_{min})/(R_{max} - R)]$, where K_d for the fura-2-Ca^{2+} complex is 224 nM; R is the fluorescence ratio (F_{340}/F_{380}); R_{max} and R_{min} are the maximal and minimal fluorescence ratios measured by addition of 10 μM of Ca^{2+} ionophore ionomycin to Ca^{2+}-replete solution (2.5 mM $CaCl_2$) and Ca^{2+}-free solution (5 mM EGTA), respectively; and β is the fluorescence ratio at 380-nm excitation determined at R_{min} and R_{max}, respectively (27, 58).

Ultrasound (Rich-Mar Sonitron 2000) and Optison (Perflutren protein type A microspheres) (51, 55) were employed to deliver NAADP into CASMCs for determination of its effect on $[Ca^{2+}]_i$. To enwrap NAADP in Optison, NAADP solution was mixed well with the Optison reagent in a volume ratio of 1:10 and incubated for 1 min (51, 55). After this mixture was added to the Ca^{2+}-free Hanks' buffer (pH 7.4) for a final concentration of NAADP at 100 nM, CASMCs were treated with ultrasound for 1 min (1 W/cm^2) (51, 55). Before and after the ultrasound treatment, Ca^{2+} fluorescence assay was performed. The untreated CASMCs were also applied to ultrasound microbubble treatment for each group as a control. To determine the effects of bafilomycin A1 (Baf) or Rya on ET-1- or NAADP-induced Ca^{2+} response, CASMCs were pretreated with 100 nM Baf or 50 μM Rya for 30 min.

The ratio of fura-2 emissions, when excited at the wavelengths of 340 and 380 nm, was recorded with a digital camera (Nikon Diaphoto TMD Inverted Microscope). Metafluor imaging and analysis software were used to acquire, digitize, and store the images for off-line processing and statistical analysis (Universal Imaging).

Planar lipid bilayer analysis of NAADP effect on SR RyR Ca^{2+} release channels. The preparation of SR-enriched microsomes from bovine coronary arteries and reconstitution of these SR membranes into a planar lipid bilayer was performed by the protocol described previously (45, 54), with cesium used as the charge carrier. The Ca^{2+} release channel activity was detected in a symmetrical 300 mM cesium methanesulfonate and 10 mM MOPS solution (pH 7.2). An Integrating Bilayer Clamp Amplifier (Model BC-525C, Warner Instrument) was used to record single-channel currents. The amplifier output signals were filtered at 1 kHz with an eight-pole Bessel Filter (Frequency Devices). Currents were digitized at a sampling rate of 10

kHz. Data acquisition and analysis were performed with pClamp software (version 8, Axon Instruments). Channel open probability (NP_o) in the lipid bilayer was determined from recordings of 3–5 min as described previously in our patch-clamp studies (45, 54). All lipid bilayer experiments were performed at room temperature (~20°C), because the bilayer system will be unstable at 37°C, which plagues observations of the effects of any pharmacological interventions on channel activity (45, 54).

The effects of NAADP (100 nM) and $NADP^+$ (100 nM) on RyR Ca^{2+} (RyR/Ca^{2+}) release channels of SR were determined, and the positive controls cADPR (100 nM) and Rya (2 μM) were used to validate the experimental condition. All doses of these compounds were based on previous studies from our laboratory or others (49, 54), and all compounds were added into the *cis* solution, with currents recorded at a holding potential of −40 mV.

ET-1-induced production of NAADP. Previous studies (22) have shown that oxotremorine (Oxo) activates ADP-ribosyl cyclase via M_1 muscarinic receptors, leading to Ca^{2+} release from the SR in coronary arteries. Furthermore, Kinnear and associates (34) demonstrated that ET-1 evoked lysosomal Ca^{2+} release by NAADP and then caused a global Ca^{2+} wave. In the present study, we compared the effects of these two possible ADP-ribosyl cyclase-activating agonists. First, we examined their effects on the production of two different ADP-ribosyl cyclase products (22). In these experiments, the primary cultured CASMCs were treated with 100 nM ET-1 or 80 μM Oxo in the presence or absence of 6 mM Nicot. After the incubation at 37°C for 15 min, the cells were washed three times with Krebs buffer, and homogenates were prepared. Cell homogenates (100 μg) were used for the subsequent conversion assay. For the NAADP assay, the homogenates were incubated with 1 mM $NADP^+$ and 30 mM NA in HEPES buffer (pH 4.5) at 37°C for 60 min, whereas 1 mM Nicot guanine dinucleotide was used as the substrate for cADPR conversion rate [cyclic GDP ribose (cGDPR) conversion rate] assay in HEPES buffer (pH 7.0).

The HPLC assay of NAADP was performed according to the protocol described above. As for the cGDPR analysis, the HPLC mobile was changed to 150 mM ammonium acetate (pH 5.5) containing 5% methanol (*solvent A*) and 50% methanol (*solvent B*). The solvent system was a linear gradient of 5% *solvent B* in *A* to 30% *solvent B* in *A* over 1 min, held for 25 min, and then increased to 50% *solvent B* over 1 min with the flow rate of 0.8 ml/min. The fluorescence detector was used with excitation wavelength of 300 nm and emission wavelength at 410 nm.

Coronary artery reactivity. The vascular reactivity of bovine coronary arteries was determined as described previously (23, 61). Small intramural coronary arteries from the left anterior descending artery were carefully dissected and placed in a Krebs bicarbonate solution containing (in mM) 119 NaCl, 4.7 KCl, 1.6 $CaCl_2$, 1.17 $MgSO_4$, 1.18 NaH_2PO_4, 24 $NaHCO_3$, 0.026 EDTA, and 5.5 glucose (pH 7.4). The small coronary arteries were then passed through its lumen by a segment of hair, and the endothelium was removed by gently rotating the hair segment (22). The denuded small artery (100–200 μm inner diameter) was transferred to a water-jacketed perfusion chamber and cannulated with two glass micropipettes at their in situ length. After a 90-min equilibration period under transmural pressure of 60 mmHg, the artery was activated by 80 mM KCl until reproducible constriction was obtained. The internal diameter of the arteries was measured with a video system composed of a stereomicroscope (Leica MZ8), a charge-coupled device camera (KP-MI AU, Hitachi), a video monitor (VM-1220U, Hitachi), a video measuring apparatus (VIA-170, Boeckeler Instrument), and a video printer (UP890 MD, Sony). The arterial images were recorded continuously with a videocassette recorder (M-674, Toshiba). The internal diameter of the arteries under 80 mM KCl was used as 100% constriction, and the subsequent artery constrictive responses to different agents were expressed as a percentage of the response to 80 mM KCl.

To determine ET-1 and Oxo-induced vasoconstriction, cumulative dose-response curves of ET-1 (10^{-10}-10^{-7} M) and Oxo (10^{-8}-10^{-4} M) were conducted by measuring changes in the internal diameter, respectively. The ET-1 and Oxo were then washed out with Krebs buffer until the contractility returned to the baseline level. To further determine the effects of Baf and Nicot on the ET-1- and Oxo-induced constriction of coronary arteries, 100 nM Baf or 6 mM Nicot were incubated for 15 min, and ET-1 and Oxo cumulative dose responses were redetermined. Throughout the experiments, Krebs buffer in the bath was continuously bubbled with a gas mixture of 95% O_2-5% CO_2 and maintained at 37 ± 0.1°C.

Statistical analysis. Data were presented as means ± SE. Significance of differences in mean values within and between multiple groups was examined using an ANOVA for repeated measures, followed by Duncan's multiple-range test. $P < 0.05$ was considered statistically significant.

RESULTS

Production of NAADP in coronary arteries. Figure 1 shows a representative reverse-phase HPLC chromatogram depicting a profile of $NADP^+$ metabolites produced by coronary arterial homogenates. As shown in Fig. 1*A*, NAADP has a retention time of 18.3 min, and the unreacted $NADP^+$ has a retention time of 16.3 min. Figure 1*B* presents a concentration-dependent conversion of $NADP^+$ to NAADP by arterial homogenates. As the homogenate protein increased from 10 to 200 μg, the $NADP^+$ conversion rate was increased from 77.9 ± 5.2 to 169.9 ± 5.9 nmol/min. When compared with the activity of purified ADP-ribosyl cyclase, the amount of NAADP produced by 1 mg of coronary arterial homogenates was equal to that

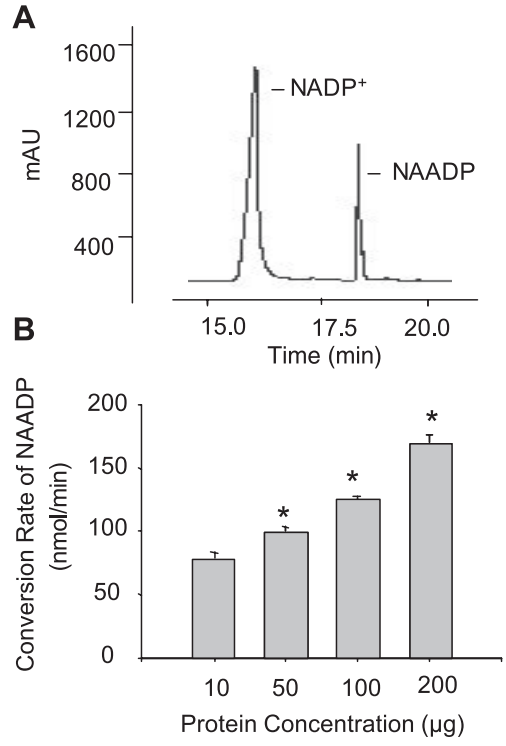

Fig. 1. HPLC analysis of nicotinic acid adenine dinucleotide phosphate (NAADP) production. *A*: typical chromatogram of $NADP^+$ and NAADP. *B*: conversion rate of $NADP^+$ into NAADP at different protein concentrations of bovine coronary arterial homogenate. *$P < 0.05$ vs. 10 μg homogenate protein group ($n = 6$ experiments). mAU, milliabsorbance unit.

produced by 5×10^{-4} ng of ADP-ribosyl cyclase. These results suggest that an enzyme responsible for the production of NAADP is present in bovine coronary arteries.

Figure 2 summarizes the maximal conversion rates of $NADP^+$ into NAADP in the homogenates, microsomes, and cytosols prepared from coronary arteries in the presence of 1 mM $NADP^+$. The conversion rates were 13.07 ± 1.17, 9.31 ± 0.81, and 18.30 ± 2.56 nmol·min^{-1}·mg protein^{-1}, respectively, in the coronary arterial homogenates, microsomes, and cytosols. It was obvious that the cytosols exhibited the highest conversion rate among three fractions of coronary preparations.

Effects of NAADP on activity of reconstituted RyR/Ca^{2+} release channels from coronary arterial muscle SR. Figure 3 shows the effects of NAADP, $NADP^+$, cADPR, and Rya on the activity of the reconstituted RyR/Ca^{2+} release channels in the planar lipid bilayer. Figure 3*A* shows representative recordings depicting the effects of NAADP, $NADP^+$, cADPR, and Rya on the activity of these Ca^{2+} release channels. Figure 3*B* summarized results showing that both NAADP and $NADP^+$ have no effects on the NP_o of the reconstituted RyR/Ca^{2+} release channels, whereas cADPR and a low concentration of Rya (2 μM) can significantly increase the NP_o of these channels. These results indicate that NAADP has no direct effect to activate RyR on the SR, as do cADPR and low doses of Rya.

Role of exogenous NAADP in inducing Ca^{2+} release response. The above results have shown that $NADP^+$ could be converted to NAADP in the coronary myocytes and that NAADP could not activate RyR/Ca^{2+} channels on the SR. Therefore, we further explored the mechanism by which NAADP increases $[Ca^{2+}]_i$ and the lysosome-related actions. As shown in Fig. 4*A*, the F340/F380 ratio was increased from 0.85 to 1.32 when 100 nM NAADP was introduced into CASMCs by an ultrasound-microbubble delivery method. In the presence of Baf, NAADP-induced Ca^{2+} release was substantially blocked. Figure 4*B* summarizes NAADP-induced alterations of $[Ca^{2+}]_i$ in the absence or presence of 100 nM Baf (n = 6 experiments). When 100 nM NAADP was introduced into CASMCs, $[Ca^{2+}]_i$ was significantly elevated from 142 ± 12 to 711 ± 47 nM. NAADP-induced Ca^{2+} release effects were reduced to 259 ± 18 nM when cells were pretreated by 100 nM Baf. However, there were no changes in basal $[Ca^{2+}]_i$ in CASMCs treated with vehicle through ultrasound and microbubble introduction.

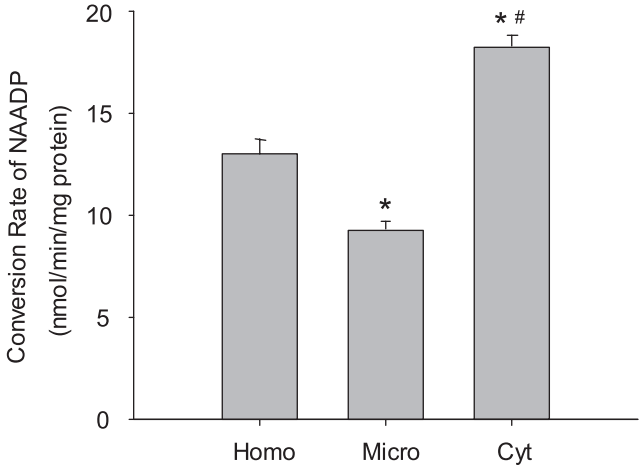

Fig. 2. Location of NAADP production. Conversion rate of NAADP in homogenate (Homo), microsome (Mico), and cytosol (Cyt) prepared from bovine coronary arteries. *$P < 0.05$ compared with Homo group; #$P < 0.05$ compared with Micro group (n = 6 experiments).

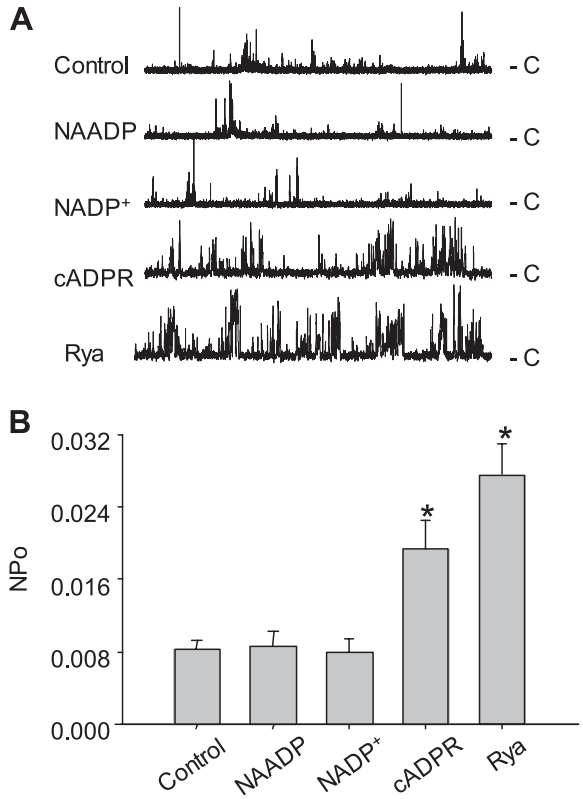

Fig. 3. Effects of NAADP (100 nM), $NADP^+$ (100 nM), cyclic ADP ribose (cADPR; 100 nM) and ryanodine (Rya; 2 μM) on activity of reconstituted Rya receptor Ca^{2+} (RyR/Ca^{2+}) release channels in planar lipid bilayer. *A*: representative recordings of channel currents trace under control condition and after addition of NAADP, $NADP^+$, cADPR, or Rya into *cis* solution with "-c" indicating closed state of channel. *B*: summarized channel open probability (NP_o) of RyR/Ca^{2+} release channels in the presence of NAADP, $NADP^+$, cADPR, and Rya, respectively. *$P < 0.05$ compared with control, NAADP, and $NADP^+$ group (n = 8 bilayers from 5 hearts).

ET-1-induced production of NAADP. By HPLC analysis, we examined whether ET-1 can enhance NAADP production in bovine coronary arteries by determining the NAADP conversion rate in CASMCs. Figure 5*A* demonstrates that ET-1 could significantly increase NAADP conversion rate in these cells from 3.69 to 5.05 nmol·min^{-1}·mg protein^{-1}, whereas Nicot, an inhibitor of ADP-ribosyl cyclase, almost completely blocked this effect. Oxo had no effect on the NAADP conversion rate compared with that of the control. In contrast, as shown in Fig. 5*B*, ET-1 had no effect on the cGDPR conversion, whereas Oxo could markedly enhance the cGDPR production. Nicot also exerted profound inhibitory effects on the Oxo-induced cGDPR conversion.

Role of endogenous NAADP in mediating ET-1-induced Ca^{2+} release response. Figure 6*A* shows several images of the fura-2 fluorescence ratio F340/F380 recorded in CASMCs treated by ET-1 (100 nM) with or without pretreatment of Baf (100 nM) or Rya (50 μM). A spatially localized Ca^{2+} burst around cell boundary precedes the global Ca^{2+} increase, as indicated by the change of red color within the cell in the

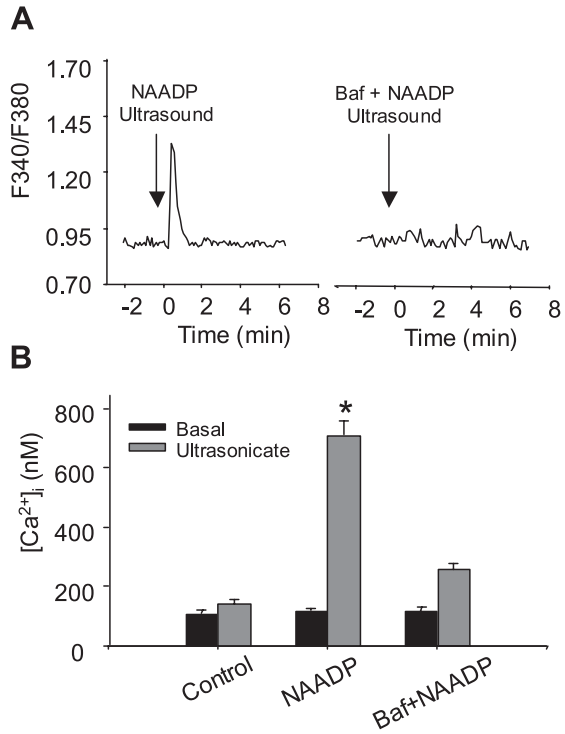

Fig. 4. Exogenous NAADP (100 nM)-induced Ca^{2+} release in primary cultured coronary arterial smooth muscle cells (CASMCs) in the absence or presence of bafilomycin A1 (Baf; 100 nM). *A*: an online recording of fura-2 fluorescence ratio of F340 vs. F380 (F340/F380) against time after treatment of NAADP or Baf plus NAADP with ultrasound and microbubble optison. *B*: effects of NAADP and Baf plus NAADP on intracellular Ca^{2+} concentration ($[Ca^{2+}]_i$). *$P < 0.05$ vs. control and Baf + NAADP group ($n = 6$ experiments).

ET-1-treated group. In the Baf-pretreated group, both the Ca^{2+} burst in the area under the cell membrane and global Ca^{2+} increases were significantly decreased, whereas in the Rya-pretreated group, only the global increase in intracellular Ca^{2+} was selectively blocked. Figure 6*B* shows a digitally converted recording of the fura-2 fluorescence ratio F340/F380 against time for $[Ca^{2+}]_i$. Consistent with fluorescence images shown above, there were two peaks when CASMCs were treated with ET-1, with a small peak at 1 min corresponding to a local $[Ca^{2+}]_i$ burst and a big peak around 3 min representing the global $[Ca^{2+}]_i$ increase or release of Ca^{2+} from the SR. When the cells were pretreated with Baf, both peaks were almost completely abolished. In the presence of a high concentration of Rya (50 μM), a RyR/Ca^{2+} release inhibitor, only the large peak of Ca^{2+} increase was substantially blocked, whereas early small peak remained. Figure 6*C* summarized ET-1-induced $[Ca^{2+}]_i$ fluctuations in the absence or presence of Baf or Rya. It is clear that there were no differences among the basal level of $[Ca^{2+}]_i$ in all the three groups, namely ET-1, Baf, and Rya treatment groups. ET-1 produced significant increases in $[Ca^{2+}]_i$ from 151 ± 43 nM of the basal level to 529 ± 32 nM at the first small Ca^{2+} transient peak, followed by a large increase of 1,815 ± 84 nM 3 min after the addition of ET-1. In the presence of 100 nM Baf, this ET-1-induced two-phase Ca^{2+} response was significantly attenuated. In contrast, Rya only significantly blocked the ET-1-induced large global Ca^{2+} increase, but it had no effect on the early small Ca^{2+} response to ET-1.

Effects of Baf and Nicot on the ET-1-induced constriction of bovine coronary artery. Figure 7*A* presents some typical microscopic photomicrographs showing coronary artery reactivity to ET-1 in the absence and presence of Baf or Nicot. ET-1 was found to induce coronary vasoconstriction, which was attenuated by either Baf or Nicot. As summarized in Fig. 7*B*, ET-1 (10^{-11}-10^{-7} M) produced a dose-dependent constriction in the freshly isolated and pressurized small coronary arteries, which was significantly attenuated by 6 mM Nicot or 100 nM Baf, respectively. As a comparison, Oxo-induced vasoconstriction was significantly blocked by Nicot but not by Baf (Fig. 7*C*). However, neither Nicot nor Baf itself had any vasoconstrictor effects on the prepressurized coronary artery (data not shown).

DISCUSSION

The present study demonstrated that *1*) an enzymatic pathway for NAADP production is present in coronary arteries, *2*) NAADP had no direct effect on RyR because it did not alter the activity of the reconstituted channels from coronary arterial smooth muscle SR, *3*) NAADP-stimulated Ca^{2+} release was blocked by a lysosome function inhibitor, and *4*) ET-1 increased the conversion of $NADP^+$ into NAADP in CASMCs

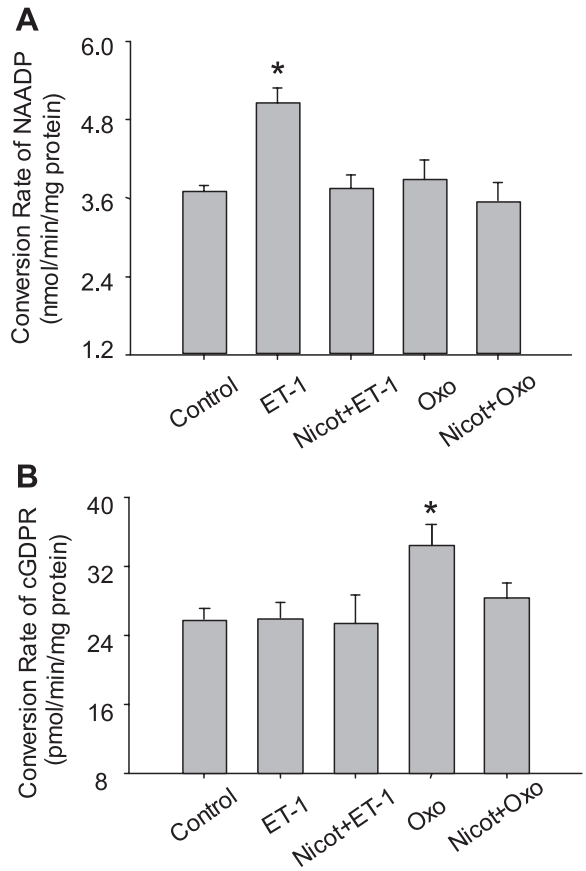

Fig. 5. HPLC assay of NAADP and cyclic GDP ribose (cGDPR) conversion rate in primary cultured CASMCs. *A*: NAADP conversion rate under endothelin-1 (ET-1; 100 nM) and oxotremorine (Oxo; 80 μM) treatment in the absence or presence of nicotinamide (Nicot; 6 mM). *B*: cGDPR conversion rate under ET-1 (100 nM) and Oxo (80 μM) treatment in the absence or presence of Nicot (6 mM). *$P < 0.05$, ET-1 group vs. other group (*A*), or Oxo group vs. other group (*B*) ($n = 6$ experiments).

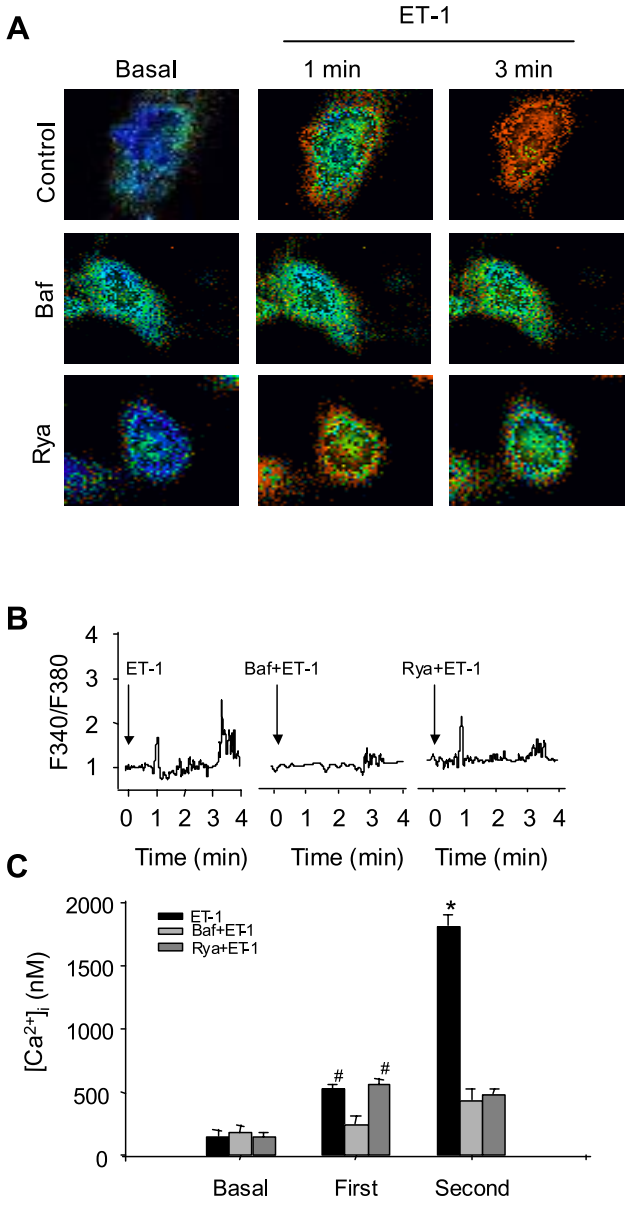

Fig. 6. ET-1 induced Ca^{2+} release response in the absence or presence of Baf and Rya. *A*: serial images of fura-2 fluorescence ratio F340/F380 recorded in primary cultured CASMCs with treatment of ET-1 (100 nM), Rya (50 μM), or Baf (100 nM). Spatially localized Ca^{2+} burst (First) around the cell boundary precedes global Ca^{2+} wave (Second) in ET-1-treated group with a significantly blocking effect in both Baf- and Rya-pretreated group. *B*: fura-2 fluorescence ratio against time. *C*: summary of results. #$P < 0.05$ vs. basal; *$P < 0.05$ vs. Baf- or Rya-pretreated group ($n = 6$ experiments).

and induced an increase in $[Ca^{2+}]_i$ and vasoconstrictor response through a NAADP-lysosome dependent mechanism.

Production of NAADP in coronary arterial myocytes. In 1987, Lee and his associates (16) reported that the metabolites of $NADP^+$ had Ca^{2+}-releasing effects from sea urchin egg microsomes. This $NADP^+$ metabolite was later identified as NAADP (6, 10, 12, 31). It has been demonstrated that a soluble protein, ADP-ribosyl cyclase, and its membrane-bound homologous CD38 are involved in the production of NAADP (1). Both of the enzymes can exchange the terminal Nicot group of the $NADP^+$ with NA to produce NAADP under the reaction of transglycosylation, which has been demonstrated in a variety of cells and tissues, including sea urchin eggs, pancreatic acinar cells, human T lymphocytes, rat brain, and rat smooth muscle cells (21, 22, 41, 45). In addition to the production of NAADP, ADP-ribosyl cyclase and CD38 are also responsible for the synthesis of cADPR with the substrate of NAD^+ by a cyclizing reaction. The enzymatic production of cADPR and the cADPR signaling pathway have been well characterized in a variety of tissues and cells (2, 19, 26, 28, 29). Recent works in our laboratory have demonstrated that this cADPR-mediated Ca^{2+} signaling is present in cardiovascular tissues, such as the myocardium, renal microvessel, and coronary arteries (21–23, 43, 59). However, so far little is known about the production

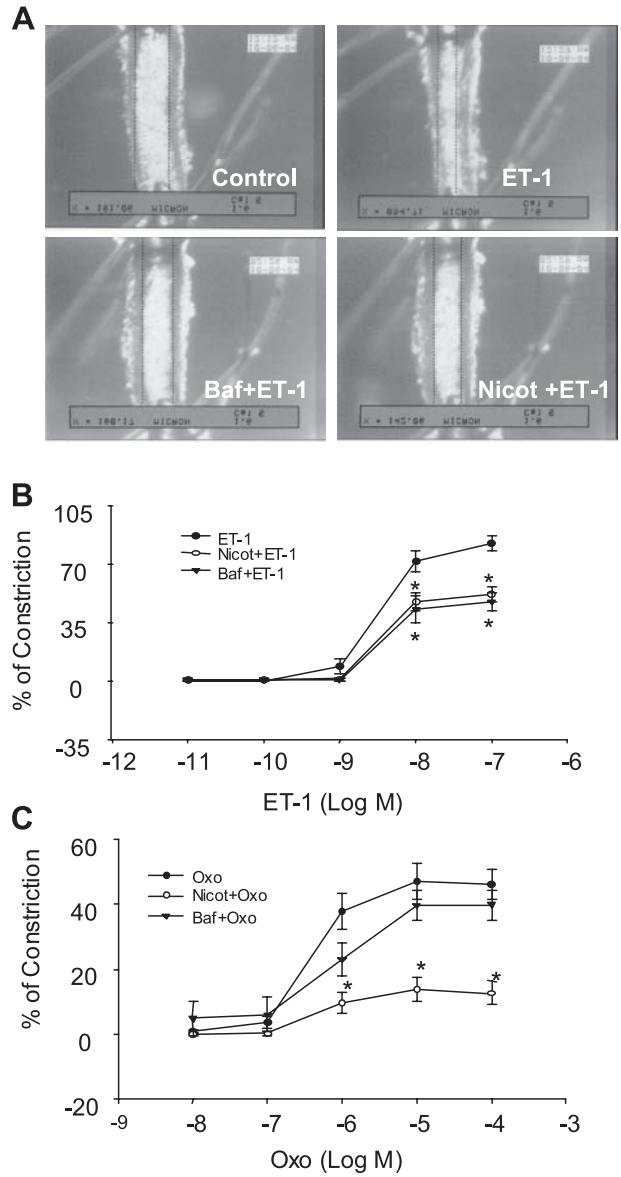

Fig. 7. ET-1-induced bovine coronary artery constriction in the absence or presence of Baf or Nicot. *A*: typical microscopic recording of ET-1-induced coronary artery constriction under different treatment. *B* and *C*: summarized results showing effects of Nicot (6 mM) or Baf (100 nM) on ET-1 (10^{-10}-10^{-7} M) and Oxo (10^{-8}-10^{-4} M)-induced vasoconstriction. *$P < 0.05$ vs. ET-1 alone-treated group (*B*) or Oxo alone-treated group (*C*) ($n = 6$ arterial preparations from different hearts).

and action of NAADP in coronary circulation. Given the peculiar properties of ADP-ribosyl cyclase and its ability to produce both cADPR and NAADP, we wondered whether NAADP could also be synthesized in the coronary artery and participate in the regulation of coronary arteral vascular tone or vasomotor response.

In the present study, HPLC analysis showed that the homogenates from bovine coronary arterial smooth muscle converted $NADP^+$ into NAADP in a concentration-dependent manner under a reaction condition of pH 4.5, which had similar efficiency to that observed for cADPR production under pH 7.4 (21, 22). These results provide the first direct evidence indicating that NAADP is an enzymatic product of $NADP^+$ in coronary arterial smooth muscle. To determine the localization of NAADP production in coronary arterial smooth muscle, we further prepared microsomes and cytosols from the coronary arteries and determined NAADP production in different fractions. When compared with homogenates, NAADP conversion rate was higher in the cytosol but lower in microsomes. It seems that NAADP production may primarily be an event that occurs in cytosol of CASMCs. Although two membrane-bound ADP-ribosyl cyclases, CD38 and CD157, and a cytosolic soluble ADP-ribosyl cyclase isoform were reported (39, 53), our previous studies demonstrated that cytosolic ADP-ribosyl cyclase activity may be primarily derived from internalized CD38 in coronary arterial smooth muscle. In addition, other studies (11, 30, 62) also demonstrated that CD38 internalization is of importance in mediating cADP-ribose production in cell cystosols. Therefore, based on current understanding, a high level of ADP-ribosyl cyclase activity to convert $NAAP^+$ to NAADP may be associated with the internalization of a membrane-bound enzyme. This internalized cytosolic ADP-ribosyl cyclase is responsible for catalyzing the exchange of the Nicot group of $NADP^+$ with NA to produce NAADP under acidic conditions.

NAADP-induced Ca^{2+} release. Previous studies (25, 32, 35, 47) reported that NAADP possibly acts on RyRs on the SR to release Ca^{2+}. These results were mostly based on pharmacological blockade or activation. There is no direct evidence that NAADP can activate RyRs. In previous studies, we demonstrated that cADPR directly activated RyR/Ca^{2+} release channels on the SR of coronary arterial smooth muscle by reconstituted lipid bilayer methods (54). This effect of cADPR on SR RyR/Ca^{2+} release channels is related to the dissociation of FKBP12.6 from RyRs (54). Therefore, we wondered whether NAADP also stimulates Ca^{2+} release in coronary arterial myocytes through its action on RyR as does cADPR. To explore this possiblity, we performed lipid bilayer reconstitution experiments using the isolated SR from coronary arterial smooth muscle. It was found that NAADP had no effect on the activity of reconstituted RyR/Ca^{2+} release channels from coronary arterial SR, suggesting that NAADP could not directly activate Ca^{2+} release from the SR in coronary arterial myocytes and that the SR RyR/Ca^{2+} release channels are not a target for the action of NAADP to produce Ca^{2+} release. Studies (34) from other laboratories demonstrated that NAADP evoked highly localized intracellular Ca^{2+} signals by mobilizing Ca^{2+} from thapsigargin (a SR Ca^{2+}-ATPase inhibitor)-insensitive stores and that heparin and high-dose Rya [inhibitors of Ins(1,4,5)P_3 and RyRs on the SR, respectively] had no inhibitory effects on NAADP-initiating local Ca^{2+} wave. Taken together, these results reveal an important fact that NAADP-induced Ca^{2+} release is independent of its direct effect activating RyR/Ca^{2+} channels in coronary arterial myocytes.

To further explore the mechanism mediating the action of NAADP and to determine the functional role of NAADP in the regulation of $[Ca^{2+}]_i$ in coronary arterial myocytes, we performed several series of experiments to determine the actions of exogenous and endogenous NAADP in increasing $[Ca^{2+}]_i$. It was found that NAADP produced a rapid Ca^{2+} release response when introduced into CASMCs by ultrasound microbubble delivery technique. This NAADP-induced Ca^{2+} release response was blocked by inhibition of lysosomal Ca^{2+} release and vacuolar proton pump function with Baf. These results indicate that NAADP is able to mobilize intracellular Ca^{2+}, which may be associated with lysosome function.

Although the present study demonstrates that a lysosome-associated mechanism may be importantly involved in NAADP-induced Ca^{2+} release, there are some other reports indicating that NAADP may induce Ca^{2+} release through other mechanisms. In this regard, it seems that the controversy is dependent on the cell or tissue types used in different experiments. For example, in early studies using the sea urchin eggs or pancreatic acinar cells, NAADP was demonstrated to mobilize Ca^{2+} from a store that is distinct pharmacologically and physically from the Ins(1,4,5)P_3- and cADPR-sensitive Ca^{2+} stores (7, 14). However, recent studies (18) in T lymphocytes and other cells have demonstrated that the Ca^{2+} release channel sensistive to NAADP in these cells is the RyR. There is also evidence that NAADP could directly activate isolated RyRs reconstituted in lipid bilayers from rabbit skeletal muscle (RyR1) (32) and cardiac microsomes (RyR2) (48). In addition, many studies have found that NAADP-induced Ca^{2+} release rarely operates in isolation but rather in combination with other pathways or factors. It is often observed that the resultant Ca^{2+} signals evoked by NAADP are boosted by Ca^{2+} release via activation of RyRs, IP_3Rs, or both (14, 15, 24, 36, 40). Now two models for the role of NAADP in inducing Ca^{2+} release have been proposed to interpret the results obtained from different cells (56). In the first model, the endoplasmic reticulum (ER) or SR expressing IP_3Rs and RyRs as a single pool is responsible for the action of NAADP. To induce Ca^{2+} release, NAADP interacts either directly with RyRs or via a separate protein that may indirectly activate RyRs (18, 25). This model can be clearly used to explain the results obtained from T lymphocytes, where NAADP-evoked release can be abolished by either RyR blockers or thapsigargin. A second model describes a two-pool or trigger hypothesis, which is based on the assumption that a NAADP-sensitive Ca^{2+} store exists, which is possibly a thapsigargin-insensitive acidic store (15). This NAADP-sensitive Ca^{2+} store is responsible for a localized signal, which is amplified by CICR through IP_3Rs and RyRs on the ER to produce a large global Ca^{2+} increase (7, 8, 13, 14). If NAADP induces Ca^{2+} release through this mechanism, a localized NAADP-induced signal would persist in the presence of IP_3Rs and RyR antagonists or thapsigargin, but it could be abolished by agents that dissipate storage of some acidic organelles, such as the vacuolar H^+ pump inhibitor, Baf, or a disruptor of lysosomal-related organelles, glycyl-phenylalanyl-naphthylamide (56). As discussed above, in CASMCs, NAADP may exert its Ca^{2+} mobilizing action

through the mechanism described in *model 2*, because NAADP did not alter the SR RyRs/Ca^{2+} release channel activity and inhibition of lysosome function abolished the effect of NAADP.

Involvement of NAADP in ET-1-induced Ca^{2+} response in CASMCs and coronary vasoconstriction. The next questions we addressed are whether and how endogenous NAADP play a role in mediating physiological response of coronary arterial muscle. ET-1 is an important endothelium-derived vasoconstrictor. ET-1 exerts a wide spectrum of biological effects on smooth muscle cells via ET_A and ET_B receptors, including inhibition of voltage-gated K^+ channels, activation of L-type Ca^{2+}, as well as mobilization of intracellular Ca^{2+} (4, 17, 20). Recent studies (34) have indicated that ET-1 exerts its Ca^{2+} mobilizing action in pulmonary arteries through a lysosome-associated Ca^{2+} activation via NAADP. In the present study, we demonstrated that ET-1 significantly increased the conversion of $NADP^+$ into NAADP in coronary arterial myocytes, indicating that NAADP may serve as a signaling messenger to produce ET-1-induced mobilization of intracellular Ca^{2+} in coronary arterial myocytes and vasoconstriction. Indeed, Ca^{2+} fluorescence imaging analysis demonstrated that ET-1 induced a sequential two-phase increase in $[Ca^{2+}]_i$ in CASMCs. The first phase Ca^{2+} spike occurred 1 min after ET-1 was added into the bath solution, and the second phase Ca^{2+} transient occurred 3 min later, which is strong and represents a global increase in $[Ca^{2+}]_i$. In the presence of Baf, both phases of Ca^{2+} response were markedly attenuated. However, a relatively high concentration of Rya, which is reported to be a classic inhibitor of SR RyR/Ca^{2+} channels, only abolished the late Ca^{2+} increase that functionally was related to Ca^{2+} release from SR Ca^{2+} stores. These results suggest that ET-1 may first stimulate Ca^{2+} release from lysosomes through NAADP action and then activate Ca^{2+} release from the SR via RyRs-sensitive CICR mechanism. This further supports the view that NAADP serves as a trigger or initiating factor to mediate ET-1-induced Ca^{2+} release from the lysosome, whereby the subsequent large Ca^{2+} release from the SR is evoked via a CICR mechanism by activation of RyRs.

To further address the functional significance of this NAADP-lysosome Ca^{2+} signaling, bovine coronary vascular reactivity to ET-1 was examined in the absence and presence of lysosome H^+-ATPase inhibitor Baf and ADP-ribosyl cyclase inhibitor Nicot. It was found that ET-1 produced dose-dependent vasoconstriction in isolated and perfused coronary arteries, which was significantly attenuated by inhibition of ADP-ribosyl cyclase or lysosomal Ca^{2+} release. However, Oxo-induced coronary arterial constriction was only attenuated by Nicot but not by Baf. This action of Oxo is consistent with those in our previous studies that cADPR was involved in the Oxo-induced coronary arterial constriction and that the cADPR-mediated Ca^{2+} release is associated with thapsigargin-sensitive Ca^{2+} pool in the SR. In addition, these results were also consistent with the findings discussed above that NAADP was an endogenous enzymatic product of ADP-ribosyl cyclase in response to ET-1 in coronary arterial preparation and that NAADP mobilized Ca^{2+} in arterial smooth muscle cells via lysosome-related mechanism. Taken together, these functional results indicate that the lysosomal Ca^{2+}-mobilizing action of NAADP plays a crucial role in ET-1-induced vasoconstrictor response in coronary arteries.

In summary, the present study demonstrated that *1*) ET-1 activated ADP-ribosyl cyclase, leading to the production of NAADP under acidic conditions or acidic organelles; *2*) NAADP produced Ca^{2+} release response independently of RyRs/Ca^{2+} release channel activation; *3*) the Ca^{2+} release action of NAADP was blocked by inhibition of lysosomal function; *4*) NAADP-induced two-phase Ca^{2+} response to ET-1 was associated with lysosome Ca^{2+}-triggering action and subsequent CICR, which results in a large global increase in $[Ca^{2+}]_i$; and *5*) the lysosome-associated Ca^{2+} regulatory mechanism through NAADP participated in the coronary vasoconstrictor response to ET-1. We conclude that NAADP is important in the regulation of $[Ca^{2+}]_i$ in CASMCs and in the mediation of coronary vasoconstriction response to ET-1.

GRANTS

This study was supported by National Heart, Lung, and Blood Institute Grants HL-057244 and HL-075316.

REFERENCES

1. **Aarhus R, Graeff RM, Dickey DM, Walseth TF, and Lee HC.** ADP-ribosyl cyclase and CD38 catalyze the synthesis of a calcium-mobilizing metabolite from NADP. *J Biol Chem* 270: 30327–30333, 1995.
2. **Bai N, Lee HC, and Laher I.** Emerging role of cyclic ADP-ribose (cADPR) in smooth muscle. *Pharmacol Ther* 105: 189–207, 2005.
3. **Berg I, Potter BV, Mayr GW, and Guse AH.** Nicotinic acid adenine dinucleotide phosphate $NAADP^+$ is an essential regulator of T-lymphocyte Ca^{2+}-signaling. *J Cell Biol* 150: 581–588, 2000.
4. **Betts LC and Kozlowski RZ.** Electrophysiological effects of endothelin-1 and their relationship to contraction in rat renal arterial smooth muscle. *Br J Pharmacol* 130: 787–796, 2000.
5. **Boittin FX, Galione A, and Evans AM.** Nicotinic acid adenine dinucleotide phosphate mediates Ca^{2+} signals and contraction in arterial smooth muscle via a two-pool mechanism. *Circ Res* 91: 1168–1175, 2002.
6. **Cancela JM.** Specific Ca^{2+} signaling evoked by cholecystokinin and acetylcholine: the roles of NAADP, cADPR, and IP_3. *Annu Rev Physiol* 63: 99–117, 2001.
7. **Cancela JM, Churchill GC, and Galione A.** Coordination of agonist-induced Ca^{2+}-signalling patterns by NAADP in pancreatic acinar cells. *Nature* 398: 74–76, 1999.
8. **Cancela JM, Gerasimenko OV, Gerasimenko JV, Tepikin AV, and Petersen OH.** Two different but converging messenger pathways to intracellular Ca^{2+} release: the roles of nicotinic acid adenine dinucleotide phosphate, cyclic ADP-ribose and inositol trisphosphate. *EMBO J* 19: 2549–2557, 2000.
9. **Cancela JM, Van Coppenolle F, Galione A, Tepikin AV, and Petersen OH.** Transformation of local Ca^{2+} spikes to global Ca^{2+} transients: the combinatorial roles of multiple Ca^{2+} releasing messengers. *EMBO J* 21: 909–919, 2002.
10. **Ceni C, Muller-Steffner H, Lund F, Pochon N, Schweitzer A, De Waard M, Schuber F, Villaz M, and Moutin MJ.** Evidence for an intracellular ADP-ribosyl cyclase/NAD^+-glycohydrolase in brain from CD38-deficient mice. *J Biol Chem* 278: 40670–40678, 2003.
11. **Chidambaram N and Chang CF.** $NADP^+$-dependent internalization of recombinant CD38 in CHO cells. *Arch Biochem Biophys* 363: 267–272, 1999.
12. **Chini EN, Beers KW, Chini CC, and Dousa TP.** Specific modulation of cyclic ADP-ribose-induced Ca^{2+} release by polyamines. *Am J Physiol Cell Physiol* 269: C1042–C1047, 1995.
13. **Churchill GC and Galione A.** NAADP induces Ca^{2+} oscillations via a two-pool mechanism by priming IP_3- and cADPR-sensitive Ca^{2+} stores. *EMBO J* 20: 2666–2671, 2001.
14. **Churchill GC and Galione A.** Spatial control of Ca^{2+} signaling by nicotinic acid adenine dinucleotide phosphate diffusion and gradients. *J Biol Chem* 275: 38687–38692, 2000.
15. **Churchill GC, Okada Y, Thomas JM, Genazzani AA, Patel S, and Galione A.** NAADP mobilizes Ca^{2+} from reserve granules, lysosome-related organelles, in sea urchin eggs. *Cell* 111: 703–708, 2002.

16. **Clapper DL, Walseth TF, Dargie PJ, and Lee HC.** Pyridine nucleotide metabolites stimulate calcium release from sea urchin egg microsomes desensitized to inositol trisphosphate. *J Biol Chem* 262: 9561–9568, 1987.
17. **Curtis TM and Scholfield CN.** Evidence for two endothelin ET_A receptor subtypes in rabbit arteriolar smooth muscle. *Br J Pharmacol* 134: 1787–1795, 2001.
18. **Dammermann W and Guse AH.** Functional ryanodine receptor expression is required for NAADP-mediated local Ca^{2+} signaling in T-lymphocytes. *J Biol Chem* 280: 21394–21399, 2005.
19. **De Flora A, Zocchi E, Guida L, Franco L, and Bruzzone S.** Autocrine and paracrine calcium signaling by the CD38/NAD^+/cyclic ADP-ribose system. *Ann NY Acad Sci* 1028: 176–191, 2004.
20. **Delarue C, Jouet IR, Gras M, Galas L, Fournier A, and Vaudry H.** Activation of endothelinA receptors in frog adrenocortical cells stimulates both calcium mobilization from intracellular stores and calcium influx through L-type calcium channels. *Endocrinology* 146: 119–129, 2005.
21. **Ge ZD, Li PL, Chen YF, Gross GJ, and Zou AP.** Myocardial ischemia and reperfusion reduce the levels of cyclic ADP-ribose in rat myocardium. *Basic Res Cardiol* 97: 312–319, 2002.
22. **Ge ZD, Zhang DX, Chen YF, Yi FX, Zou AP, Campbell WB, and Li PL.** Cyclic ADP-ribose contributes to contraction and Ca^{2+} release by M_1 muscarinic receptor activation in coronary arterial smooth muscle. *J Vasc Res* 40: 28–36, 2003.
23. **Geiger J, Zou AP, Campbell WB, and Li PL.** Inhibition of cADP-ribose formation produces vasodilation in bovine coronary arteries. *Hypertension* 35: 397–402, 2000.
24. **Genazzani AA and Galione A.** A Ca^{2+} release mechanism gated by the novel pyridine nucleotide, NAADP. *Trends Pharmacol Sci* 18: 108–110, 1997.
25. **Gerasimenko JV, Maruyama Y, Yano K, Dolman NJ, Tepikin AV, Petersen OH, and Gerasimenko OV.** NAADP mobilizes Ca^{2+} from a thapsigargin-sensitive store in the nuclear envelope by activating ryanodine receptors. *J Cell Biol* 163: 271–282, 2003.
26. **Gerasimenko O and Gerasimenko J.** New aspects of nuclear calcium signalling. *J Cell Sci* 117: 3087–3094, 2004.
27. **Grynkiewicz G, Poenie M, and Tsien RY.** A new generation of Ca^{2+} indicators with greatly improved fluorescence properties. *J Biol Chem* 260: 3440–3450, 1985.
28. **Guse AH.** Biochemistry, biology, and pharmacology of cyclic adenosine diphosphoribose (cADPR). *Curr Med Chem* 11: 847–855, 2004.
29. **Guse AH.** Regulation of calcium signaling by the second messenger cyclic adenosine diphosphoribose (cADPR). *Curr Mol Med* 4: 239–248, 2004.
30. **Han MK, Kim SJ, Park YR, Shin YM, Park HJ, Park KJ, Park KH, Kim HK, Jang SI, An NH, and Kim UH.** Antidiabetic effect of a prodrug of cysteine, L-2-oxothiazolidine-4-carboxylic acid, through CD38 dimerization and internalization. *J Biol Chem* 277: 5315–5321, 2002.
31. **Hellmich MR and Strumwasser F.** Purification and characterization of a molluscan egg-specific NADase, a second-messenger enzyme. *Cell Regul* 2: 193–202, 1991.
32. **Hohenegger M, Suko J, Gscheidlinger R, Drobny H, and Zidar A.** Nicotinic acid-adenine dinucleotide phosphate activates the skeletal muscle ryanodine receptor. *Biochem J* 367: 423–431, 2002.
33. **Johnson JD and Misler S.** Nicotinic acid-adenine dinucleotide phosphate-sensitive calcium stores initiate insulin signaling in human beta cells. *Proc Natl Acad Sci USA* 99: 14566–14571, 2002.
34. **Kinnear NP, Boittin FX, Thomas JM, Galione A, and Evans AM.** Lysosome-sarcoplasmic reticulum junctions. A trigger zone for calcium signaling by nicotinic acid adenine dinucleotide phosphate and endothelin-1. *J Biol Chem* 279: 54319–54326, 2004.
35. **Langhorst MF, Schwarzmann N, and Guse AH.** Ca^{2+} release via ryanodine receptors and Ca^{2+} entry: major mechanisms in NAADP-mediated Ca^{2+} signaling in T-lymphocytes. *Cell Signal* 16: 1283–1289, 2004.
36. **Lee HC.** Mechanisms of calcium signaling by cyclic ADP-ribose and NAADP. *Physiol Rev* 77: 1133–1164, 1997.
37. **Lee HC.** Physiological functions of cyclic ADP-ribose and NAADP as calcium messengers. *Annu Rev Pharmacol Toxicol* 41: 317–345, 2001.
38. **Lee HC.** Specific binding of cyclic ADP-ribose to calcium-storing microsomes from sea urchin eggs. *J Biol Chem* 266: 2276–2281, 1991.
39. **Lee HC and Aarhus R.** ADP-ribosyl cyclase: an enzyme that cyclizes NAD^+ into a calcium-mobilizing metabolite. *Cell Regul* 2: 203–209, 1991.
40. **Lee HC and Aarhus R.** A derivative of NADP mobilizes calcium stores insensitive to inositol trisphosphate and cyclic ADP-ribose. *J Biol Chem* 270: 2152–2157, 1995.
41. **Lee HC and Aarhus R.** Functional visualization of the separate but interacting calcium stores sensitive to NAADP and cyclic ADP-ribose. *J Cell Sci* 113: 4413–4420, 2000.
42. **Lee KW, Webb SE, and Miller AL.** Ca^{2+} released via IP_3 receptors is required for furrow deepening during cytokinesis in zebrafish embryos. *Int J Dev Biol* 47: 411–421, 2003.
43. **Li P, Zou AP, and Campbell WB.** Metabolism and actions of ADP-riboses in coronary arterial smooth muscle. *Adv Exp Med Biol* 419: 437–441, 1997.
44. **Li PL, Chen CL, Bortell R, and Campbell WB.** 11,12-Epoxyeicosatrienoic acid stimulates endogenous mono-ADP-ribosylation in bovine coronary arterial smooth muscle. *Circ Res* 85: 349–356, 1999.
45. **Li PL, Tang WX, Valdivia HH, Zou AP, and Campbell WB.** cADP-ribose activates reconstituted ryanodine receptors from coronary arterial smooth muscle. *Am J Physiol Heart Circ Physiol* 280: H208–H215, 2001.
46. **Li PL, Zou AP, and Campbell WB.** Regulation of KCa-channel activity by cyclic ADP-ribose and ADP-ribose in coronary arterial smooth muscle. *Am J Physiol Heart Circ Physiol* 275: H1002–H1010, 1998.
47. **Mitchell KJ, Lai FA, and Rutter GA.** Ryanodine receptor type I and nicotinic acid adenine dinucleotide phosphate receptors mediate Ca^{2+} release from insulin-containing vesicles in living pancreatic beta-cells (MIN6). *J Biol Chem* 278: 11057–11064, 2003.
48. **Mojzisova A, Krizanova O, Zacikova L, Kominkova V, and Ondrias K.** Effect of nicotinic acid adenine dinucleotide phosphate on ryanodine calcium release channel in heart. *Pflügers Arch* 441: 674–677, 2001.
49. **Navazio L, Bewell MA, Siddiqua A, Dickinson GD, Galione A, and Sanders D.** Calcium release from the endoplasmic reticulum of higher plants elicited by the NADP metabolite nicotinic acid adenine dinucleotide phosphate. *Proc Natl Acad Sci USA* 97: 8693–8698, 2000.
50. **Nusco GA, Lim D, Sabala P, and Santella L.** Ca^{2+} response to cADPr during maturation and fertilization of starfish oocytes. *Biochem Biophys Res Commun* 290: 1015–1021, 2002.
51. **Ohta S, Suzuki K, Tachibana K, and Yamada G.** Microbubble-enhanced sonoporation: efficient gene transduction technique for chick embryos. *Genesis* 37: 91–101, 2003.
52. **Patterson RL, Boehning D, and Snyder SH.** Inositol 1,4,5-trisphosphate receptors as signal integrators. *Annu Rev Biochem* 73: 437–465, 2004.
53. **Rusinko N and Lee HC.** Widespread occurrence in animal tissues of an enzyme catalyzing the conversion of NAD^+ into a cyclic metabolite with intracellular Ca^{2+}-mobilizing activity. *J Biol Chem* 264: 11725–11731, 1989.
54. **Tang WX, Chen YF, Zou AP, Campbell WB, and Li PL.** Role of FKBP12.6 in cADPR-induced activation of reconstituted ryanodine receptors from arterial smooth muscle. *Am J Physiol Heart Circ Physiol* 282: H1304–H1310, 2002.
55. **Taniyama Y, Tachibana K, Hiraoka K, Namba T, Yamasaki K, Hashiya N, Aoki M, Ogihara T, Yasufumi K, and Morishita R.** Local delivery of plasmid DNA into rat carotid artery using ultrasound. *Circulation* 105: 1233–1239, 2002.
56. **Yamasaki M, Churchill GC, and Galione A.** Calcium signalling by nicotinic acid adenine dinucleotide phosphate (NAADP). *FEBS J* 272: 4598–4606, 2005.
57. **Yamasaki M, Masgrau R, Morgan AJ, Churchill GC, Patel S, Ashcroft SJ, and Galione A.** Organelle selection determines agonist-specific Ca^{2+} signals in pancreatic acinar and beta cells. *J Biol Chem* 279: 7234–7240, 2004.
58. **Yi FX, Zhang AY, Campbell WB, Zou AP, Van Breemen C, and Li PL.** Simultaneous in situ monitoring of intracellular Ca^{2+} and NO in endothelium of coronary arteries. *Am J Physiol Heart Circ Physiol* 283: H2725–H2732, 2002.
59. **Yu JZ, Zhang DX, Zou AP, Campbell WB, and Li PL.** Nitric oxide inhibits Ca^{2+} mobilization through cADP-ribose signaling in coronary arterial smooth muscle cells. *Am J Physiol Heart Circ Physiol* 279: H873–H881, 2000.
60. **Zhang AY, Yi F, Teggatz EG, Zou AP, and Li PL.** Enhanced production and action of cyclic ADP-ribose during oxidative stress in small bovine coronary arterial smooth muscle. *Microvasc Res* 67: 159–167, 2004.
61. **Zhang DX, Zou AP, and Li PL.** Adenosine diphosphate ribose dilates bovine coronary small arteries through apyrase- and 5′-nucleotidase-mediated metabolism. *J Vasc Res* 38: 64–72, 2001.
62. **Zocchi E, Usai C, Guida L, Franco L, Bruzzone S, Passalacqua M, and De Flora A.** Ligand-induced internalization of CD38 results in intracellular Ca^{2+} mobilization: role of NAD^+ transport across cell membranes. *FASEB J* 13: 273–283, 1999.